Supplement of Geosci. Model Dev., 18, 10095–10117, 2025
https://doi.org/10.5194/gmd-18-10095-2025-supplement

Geoscientific Model Development
Open Access
EGU

Supplement of

An emulator-based modelling framework for studying astronomical controls on ocean anoxia with an application to the Devonian

Loïc Sablon et al.

Correspondence to: Loïc Sablon (loic.sablon@uclouvain.be)

Supplement

This supplement provides additional figures referenced in the main text. It includes: (i) spatial visualisations of the principal components used by the emulator for temperature and runoff, (ii) maps comparing annual-mean temperature and runoff between contrasting orbital states (high vs. low climate precession and high vs. low obliquity), and (iii) an illustrative time series of oceanic oxygen from the GEOCLIM ocean module.

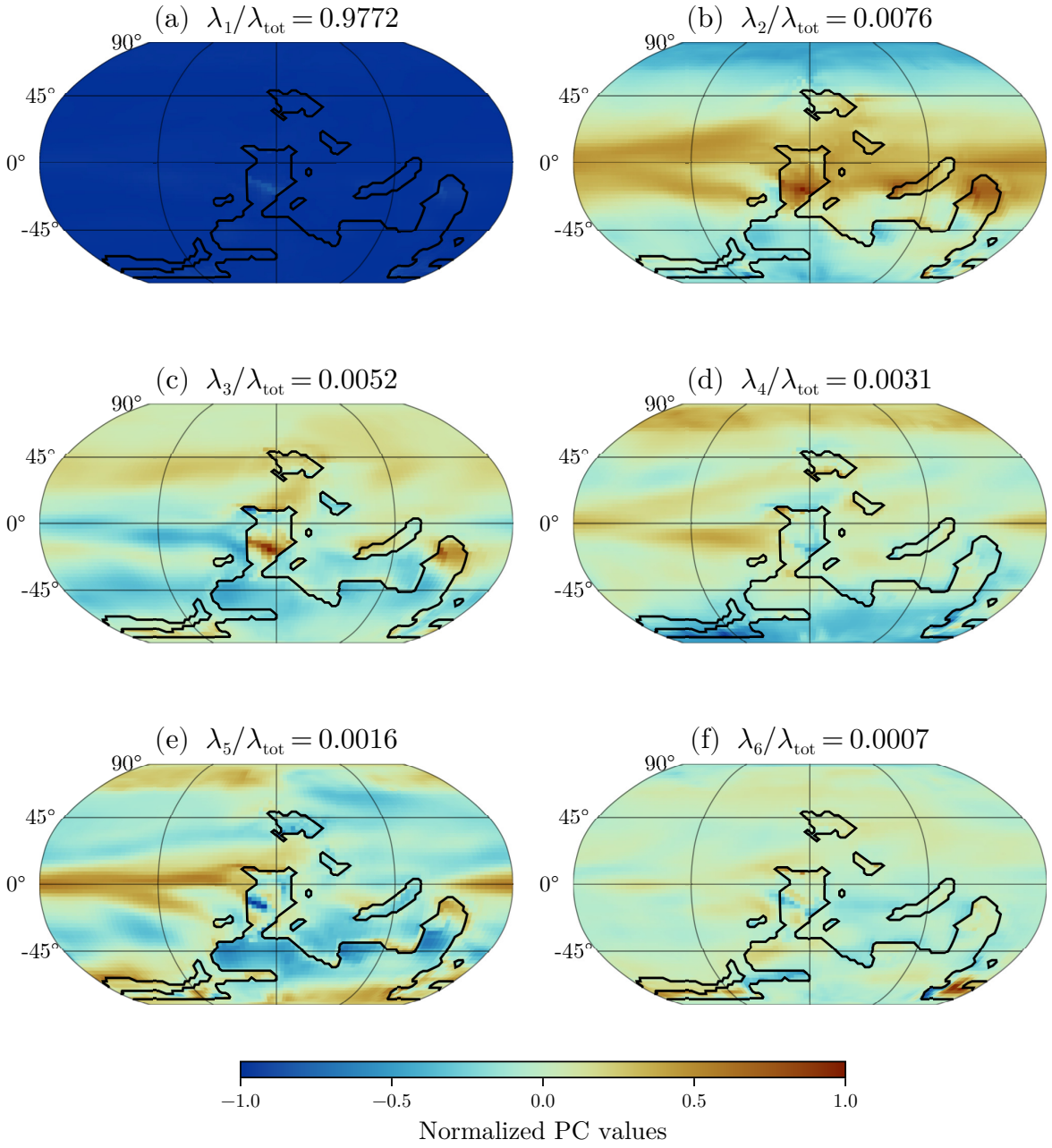

Figure S1: Principal components of annual-mean surface air temperature used by the climate emulator. The panels summarise the leading spatial modes and their relative importance (explained variance) extracted from the training dataset.

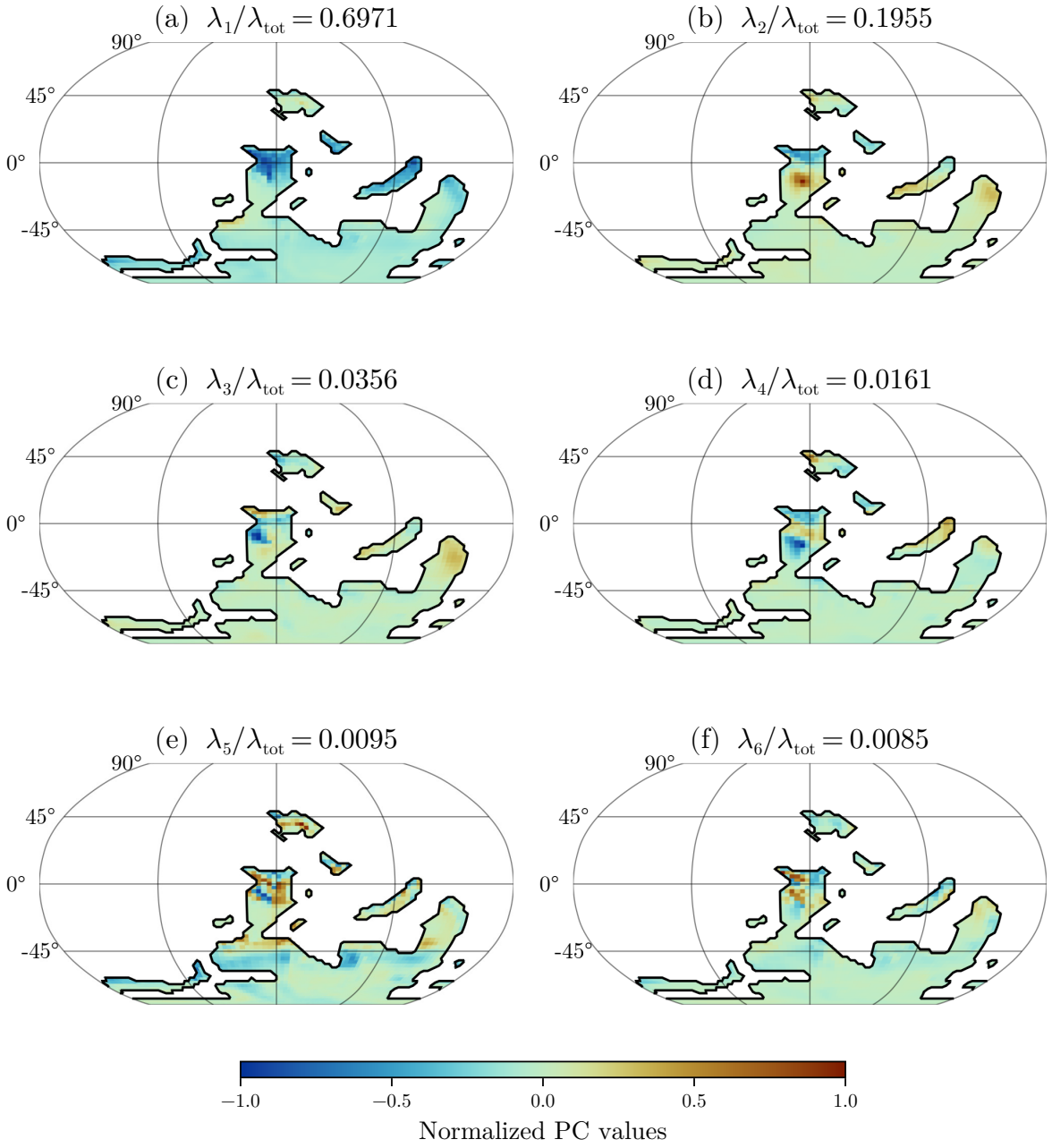

Figure S2: Principal components of annual-mean surface runoff used by the climate emulator. The panels summarise the leading spatial modes and their relative importance (explained variance) extracted from the training dataset.

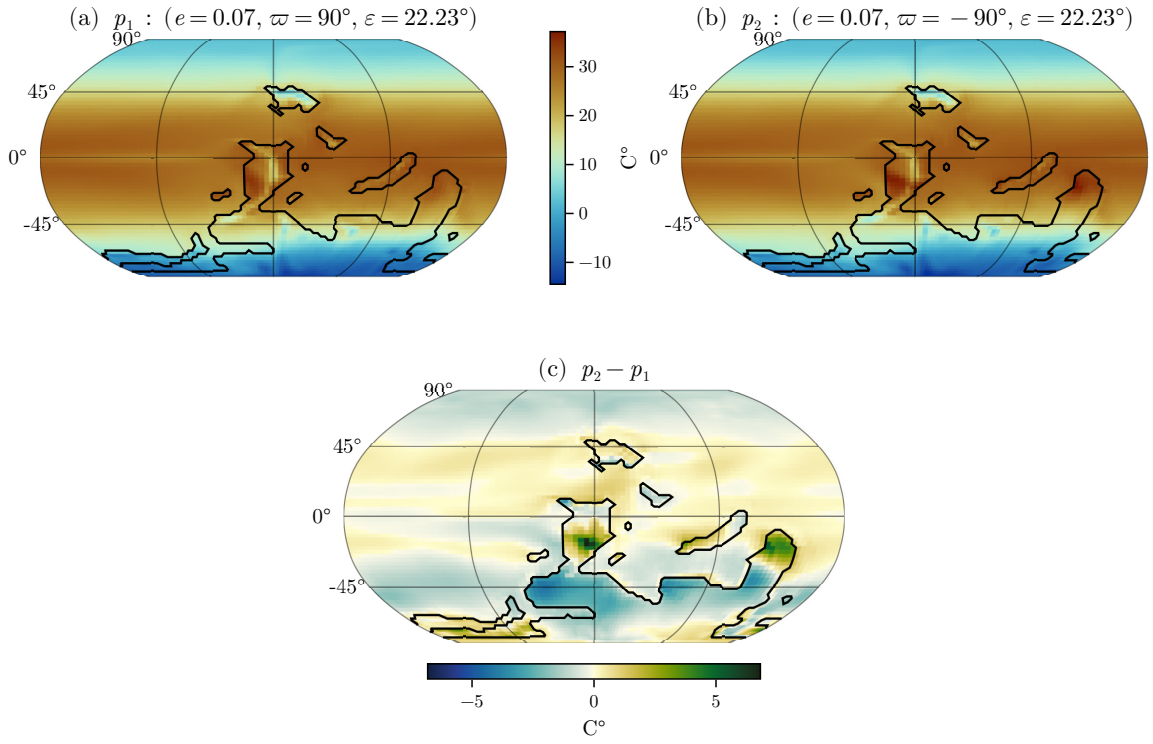

Figure S3: Contrast in annual-mean surface air temperature between two climate precession end-members. Panel (a) $\sin \varpi = 1$ vs. (b) $\sin \varpi = -1$.

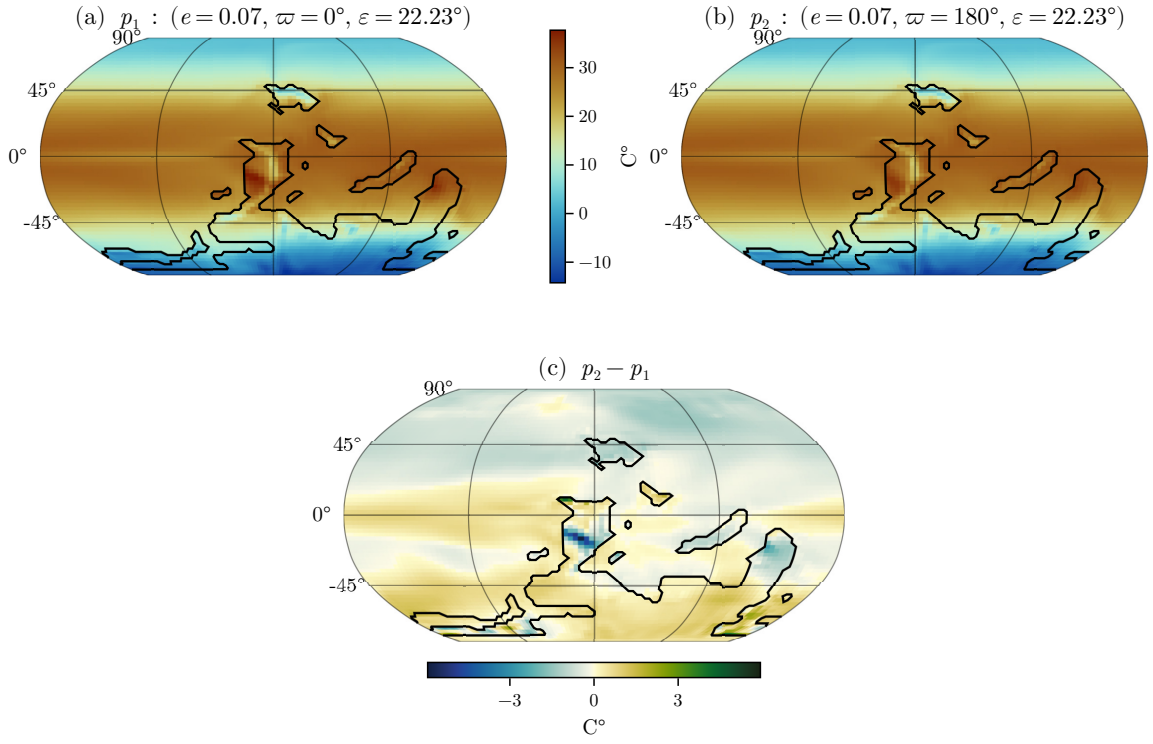

Figure S4: As in Fig. S3 but for an alternative orbital configuration with panel (a) $\cos \varpi = 1$ vs. (b) $\cos \varpi = -1$.

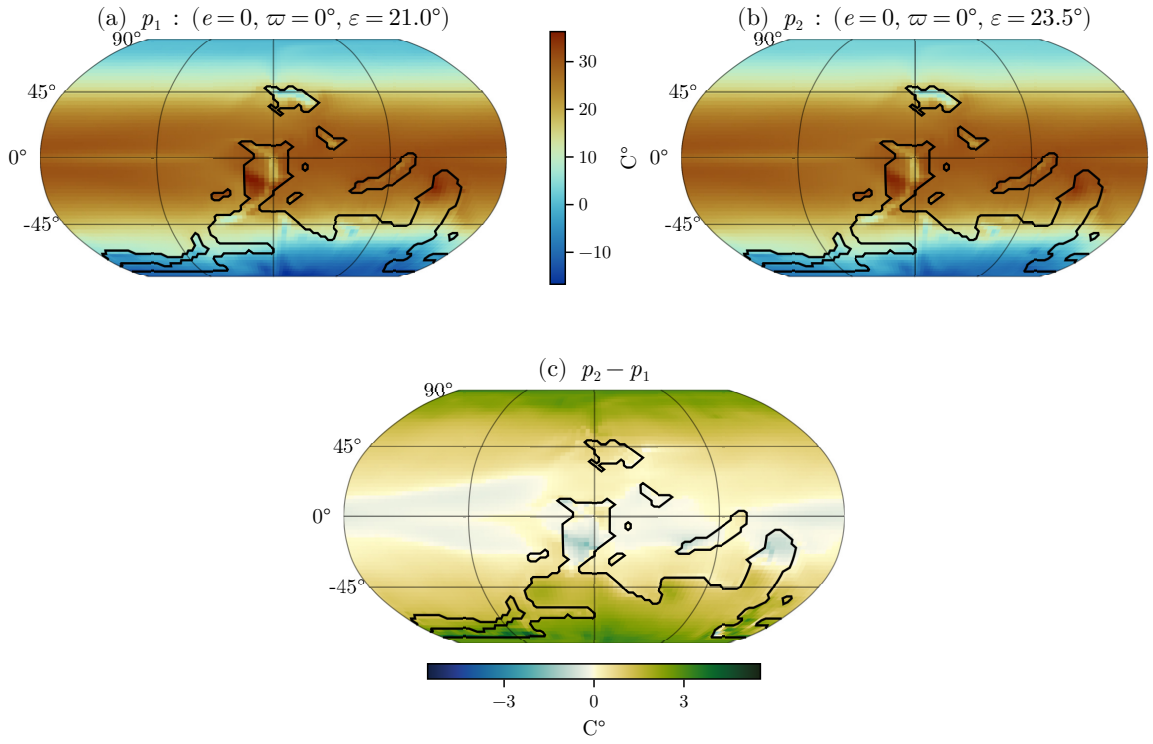

Figure S5: Contrast in annual-mean surface air temperature between low – panel (a) – and high – panel (b) – obliquity states, showing the latitudinal structure of the temperature response.

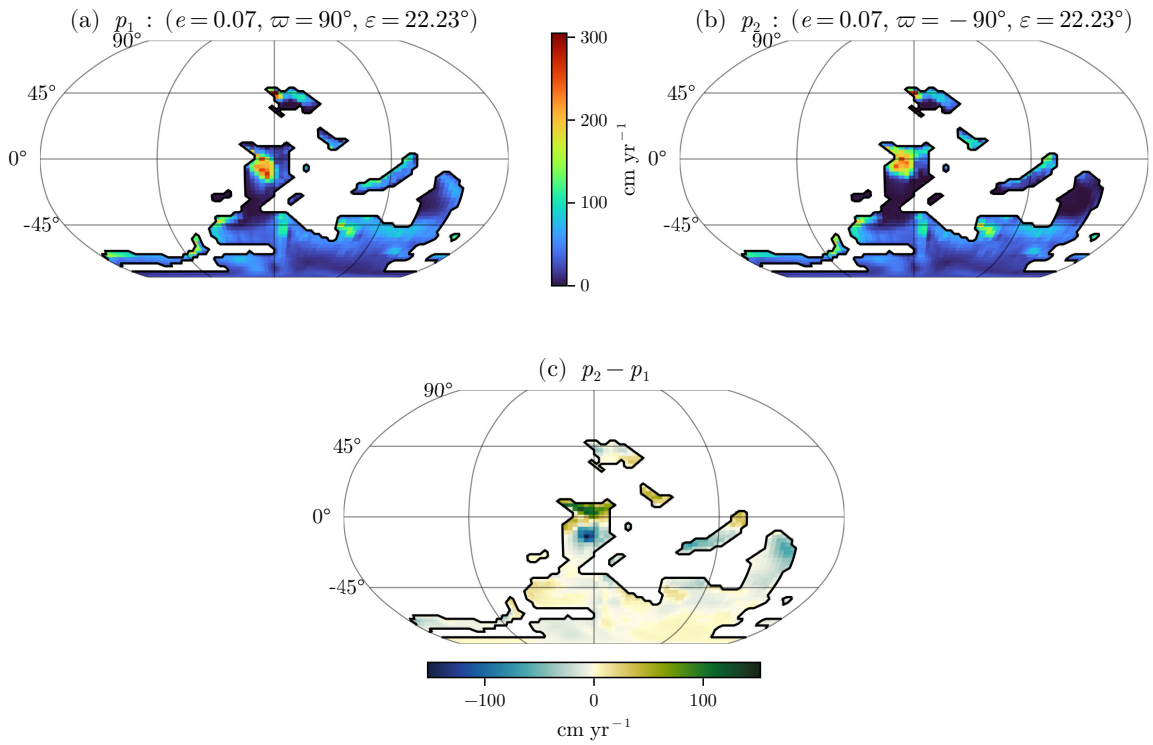

Figure S6: Contrast in annual-mean surface runoff between two climate precession end-members. Panel (a) $\sin \varpi = 1$ vs. (b) $\sin \varpi = -1$.

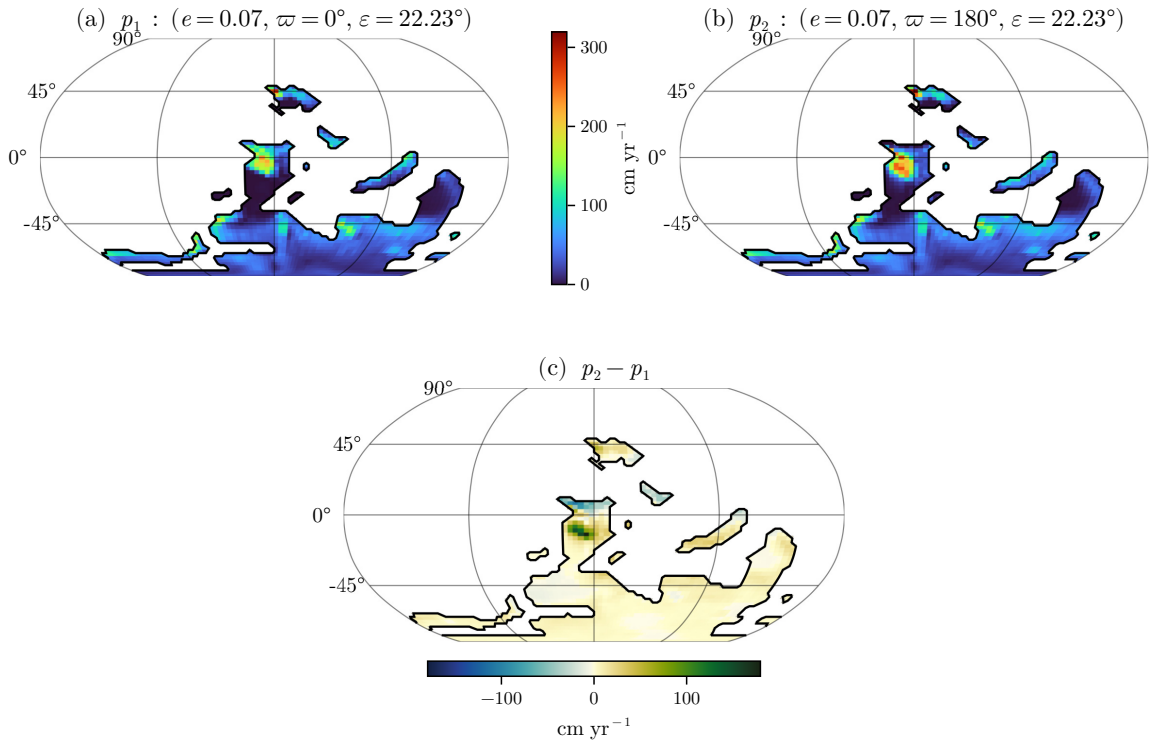

Figure S7: As in Fig. S6 but for an alternative orbital configuration, with panel (a) $\cos\varpi = 1$ vs. panel (b) $\cos\varpi = -1$.

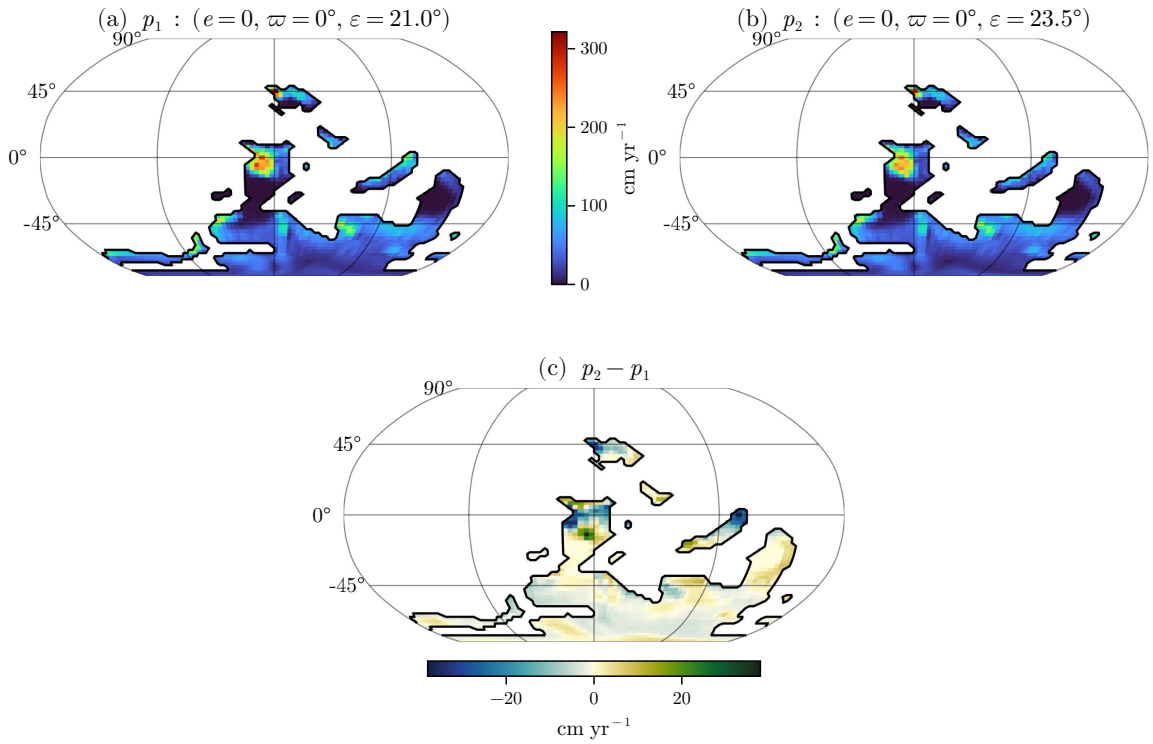

Figure S8: Contrast in annual-mean runoff between low – panel (a) – and high – panel (b) – obliquity states, showing a limited impact of obliquity on global runoff patterns when compared to precession-driven changes.

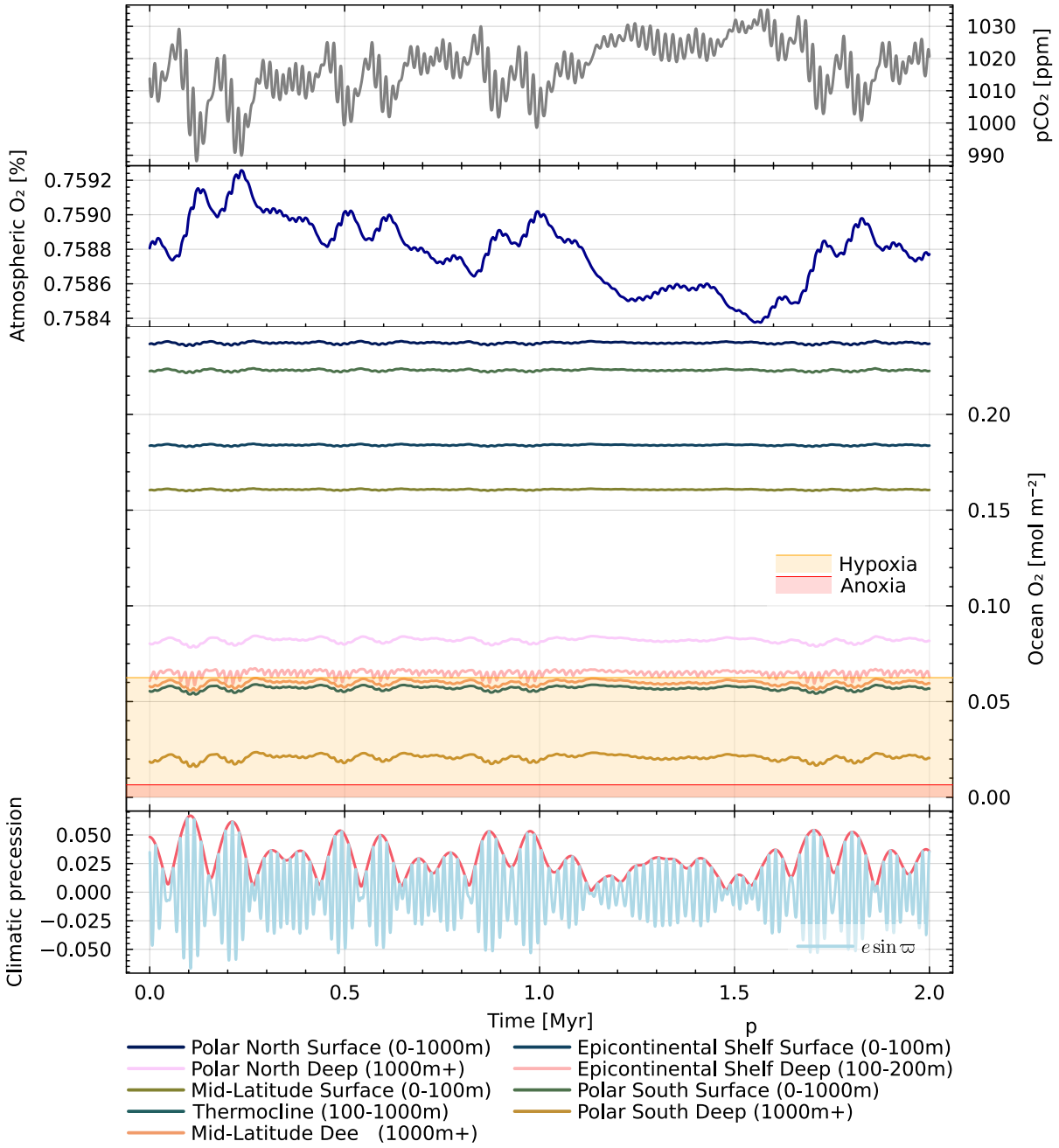

Figure S9: Illustrative time series of oceanic dissolved oxygen from the GEOCLIM ocean module for the astronomical scenario discussed in the main text. Variations are modest and consistent with the limited impact of orbital forcing on global anoxia in the present configuration. The hypoxic threshold (62.5×10^{-3} mol m−3) and anoxic threshold (6.5×10^{-3} mol m−3) following Gérard et al. (2025) are indicated for reference.